

## Characteristic Features of Edge Transport Barrier Formed in Helical Divertor Configuration of the Large Helical Device

K. Toi 1), F. Watanabe 2), S. Ohdachi 1), K. Narihara 1), T. Morisaki 1), S. Sakakibara 1), X. Gao 3), M. Goto 1), K. Ida 1), M. Kobayashi 1), S. Masuzaki 1), J. Miyazawa 1), S. Morita 1), K. Tanaka 1), T. Tokuzawa 1), K.W. Watanabe 1), A. Weller 4), L. Yan 5), M. Yoshinuma 1), K. Kawahata 1), A. Komori 1), LHD Experimental Group 1)

1) National Institute for Fusion Science, Toki, Japan

2) Department of Energy Science and Engineering, Nagoya University, Nagoya, Japan

3) Institute of Plasma Physics, Chinese Academy of Science, Hefei, China

4) Max-Planck-Institut für Plasmaphysik, D-17491 Greifswald, Germany

5) Southwestern Institute of Physics, Chengdu, China

e-mail contact of main author: [toi@lhd.nifs.ac.jp](mailto:toi@lhd.nifs.ac.jp)

**Abstract** In a helical divertor configuration of the Large Helical Device (LHD), transport barrier was formed through low to high confinement (L-H) transition in the plasma edge region including ergodic field layer of which region is in the magnetic hill. The plasma stored energy or the averaged bulk plasma beta  $\langle\beta_{\text{dia}}\rangle$  (derived from diamagnetic measurement) starts to increase just after the transition. In the case that both  $\langle\beta_{\text{dia}}\rangle$  and line-averaged electron density  $\langle n_e \rangle$  at the transition are relatively high as  $\langle\beta_{\text{dia}}\rangle \geq 1.5\%$  and  $\langle n_e \rangle \geq 2 \times 10^{19} \text{ m}^{-3}$ , the increase is hampered by rapid growth of edge MHD modes and/or small ELM like activities just after the transition. On the other hand, the transition at lower  $\langle n_e \rangle$  ( $\leq 1.5 \times 10^{19} \text{ m}^{-3}$ ) and  $\langle\beta_{\text{dia}}\rangle$  ( $< 2\%$ ) leads to a continuous increase in the stored energy with a time scale longer than the global energy confinement time, without suffering from these MHD activities near the edge. The ETB typically formed in electron density profile extends into ergodic field layer defined in the vacuum field. The width of ETB is almost independent of the toroidal field strength from 0.5T to 1.5T and is much larger than the poloidal ion gyro-radius. When resonant helical field perturbations are applied to expand a magnetic island size at the rational surface of the rotational transform  $1/2\pi=1$  near the edge, the L-H transition is triggered at lower electron density compared with the case without the field perturbations. The application of large helical field perturbations also suppresses edge MHD modes and ELM like activities.

### 1. Introduction

Formation of edge transport barrier (ETB) by L-H transition is observed in various toroidal configurations, that is, poloidal divertor and limiter configurations in tokamaks [1], and limiter and island divertor configurations in helical devices ( CHS[2-5] and W7-AS[6,7]) . Steady state sustainment of H-mode is an important issue toward burning plasma experiment. Plasma performance and global stability of ETB sensitively depend on the height and width of “pedestal” or ETB. However, a dominant control mechanism of the ETB width is not clarified yet. Understanding of control of edge localized modes (ELMs) is still insufficient, although database of ELMs is growing [8]. In particular, main concern is serious damage of

divertor plates by large amplitude singular ELM which is called type-I ELM. Recent experiment in DIII-D has demonstrated that type-I ELM can be effectively suppressed by application of resonant helical field perturbations for inducing field ergodization of a part of ETB region, without losing high plasma performance [9]. The results of DIII-D experiment suggest that fine tuning of ETB structure by the technique is essential to obtain the above favorable results. However, roles of ergodic field layer and sizable magnetic islands near the plasma edge in ETB formation are not yet fully understood on H-modes in tokamaks as well as helical devices.

The LHD has a unique magnetic configuration with helical divertor, where nested magnetic surfaces are surrounded by ergodic field layer. The L-H transition and ETB formation were observed for the first time in inward-shifted magnetic configurations such as  $R_{ax}=3.6\text{m}$  ( $R_{ax}$ : the magnetic axis position of the vacuum field) on LHD [10-12]. Effects of ergodic field layer on ELM activities are investigated using a special character of outward-shifted configurations such as  $R_{ax}=4.0\text{m}$  where ergodic field layer is considerably thick [13]. Moreover, a sizable  $m/n=1/1$  magnetic island can be forcedly generated in plasma edge region by application of resonant helical field perturbations using so-called Local Island Divertor (LID) coil [14], where  $m$  and  $n$  stand for poloidal and toroidal mode numbers, respectively. Thus, LHD has an advantage for studying roles of ergodic field layer and sizable magnetic island near the edge on L-H transition, ETB formation and ELMs.

In Fig.1, edge structure of the vacuum magnetic configuration in LHD is shown for two cases: (a) ergodic field layer in the inward-shifted configuration of  $R_{ax}=3.6\text{ m}$  and the parameter  $\gamma$  related to the plasma aspect ratio [15]  $\gamma=1.254$ , and (b) edge structure where  $m/n=1/1$  magnetic island is produced by the LID coil. In the configuration with  $\gamma=1.22$ , the size of the last closed flux surface is reduced by about 8% for the configuration of  $\gamma=1.254$  at  $R_{ax}=3.6\text{m}$ . It should be noted that in the case (b) the ergodic field layer appreciably extends toward the separatrix of the expanded  $m/n=1/1$  island, remaining a thin layer of nested magnetic surfaces of about 2 cm thickness in the horizontally elongated section.

## 2. Characteristics of L-H transition and ETB

In inward-shifted configuration of LHD ( $R_{ax}=3.6\text{m}$  and  $3.55\text{m}$ ), the L-H transition was first observed in relatively high beta plasmas of the averaged beta (derived from diamagnetic

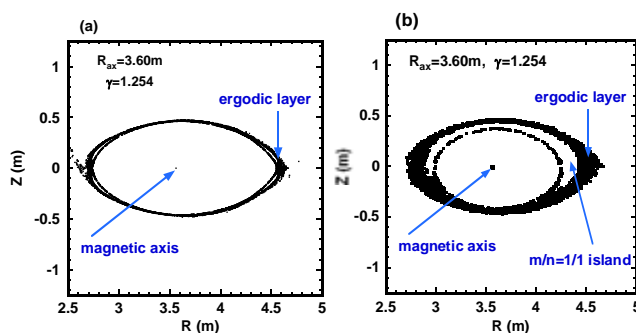


Fig.1 (a) Ergodic field layer in the configuration of  $R_{ax}=3.6\text{m}$  and  $\gamma=1.254$  in LHD. Thomson scattering data are taken in this horizontally elongated section. (b) Ergodic field layer and  $m/n=1/1$  magnetic island generated by LID field in the configuration of  $R_{ax}=3.6\text{m}$  and  $\gamma=1.254$ .

measurement)  $\langle\beta_{dia}\rangle \geq 1.5\%$  where the line averaged electron density  $\langle n_e \rangle$  is also relatively high ( $\langle n_e \rangle \geq 2 \times 10^{19} \text{ m}^{-3}$ ). On these H-mode plasmas obtained in the parameter regime, edge MHD modes are immediately excited after a short quiescent H-phase ( $< 20 \text{ ms}$ ) and interrupt the further rise in  $\langle\beta_{dia}\rangle$  in the followed H-phase [10, 11]. A shot shown in Fig.2 has similar characters to those typically observed in relatively high beta regime. In this shot, low frequency  $m/n=1/2$  edge MHD mode which would be resistive interchange modes driven

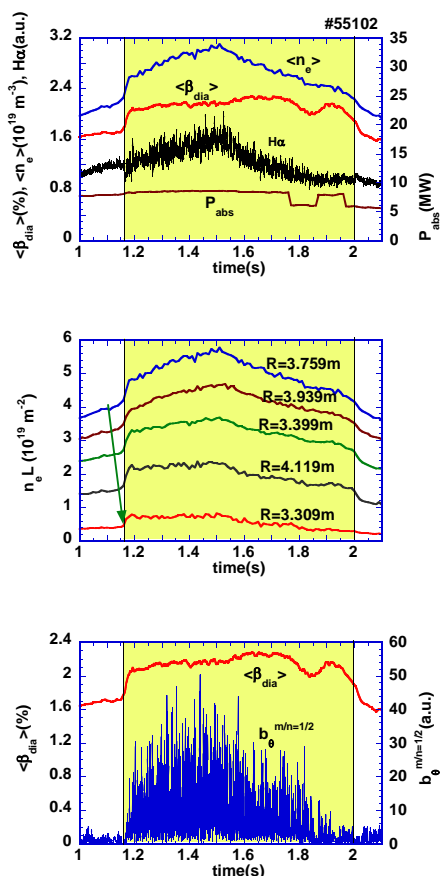


Fig.2 A typical NBI heated plasma with L-H and H-L transition where  $R_{ax}=3.6\text{m}$  and  $\gamma=1.22$  at  $Bt=-1.0T$ , where the rise in  $\langle\beta_{dia}\rangle$  is blocked by destabilization of edge MHD modes such as  $m/n=1/2$ . The arrow in the middle figure indicates the time that line integrated electron density ( $n_e L$ ) starts to rise.

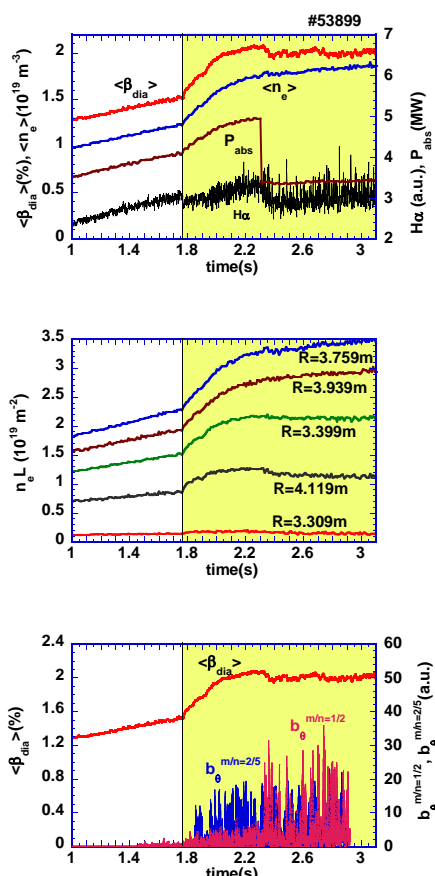


Fig.3 A relatively low density plasma where a longer rise in  $\langle\beta_{dia}\rangle$  after the L-H transition takes place, where  $Bt=-0.75T$ ,  $R_{ax}=3.6\text{m}$ , and  $\gamma=1.22$ . In this shot,  $m/n=1/2$  and  $2/5$  modes gradually increase together with  $m/n=2/3$  and  $2/4$  modes, where magnetic probe data are available to  $t\sim 2.9\text{s}$ .

by the steep pressure gradient in the magnetic hill is significantly excited, accompanying the second ( $m/n=2/4$ ) and third harmonics ( $m/n=3/6$ ). They exhibit a similar shape of frequency spectrum of magnetic fluctuations to the edge harmonic oscillations (EHOs) observed at the very edge with fairly low collisionality in quiescent double barrier H-mode on DIII-D[16], although these harmonic modes in LHD are excited in collisional edge region. The edge MHD modes do not regulate edge electron density preferentially but do edge pressure gradient there. Accordingly, they are thought to be different from EHOs. An interesting point in this shot is that the electron

density increases successively from the core to edge and then the transition occurs exhibiting a sudden rise in the edge electron density, as shown in Fig.2. Recently, the L-H transition has been achieved in relatively low density and low beta regime ( $\langle n_e \rangle \sim 1.1 \times 10^{19} \text{ m}^{-3}$  and  $\langle \beta_{\text{dia}} \rangle \sim 1\%$ ), where  $\langle \beta_{\text{dia}} \rangle$  rises continuously for longer time period ( $\sim 140 \text{ ms}$ ) without suffering from strong edge MHD modes [12]. Moreover, a continuous rise in  $\langle \beta_{\text{dia}} \rangle$  for more than 100ms just after the L-H transition is also observed in lower density plasmas ( $\leq 1.5 \times 10^{19} \text{ m}^{-3}$ ) with relatively high  $\langle \beta_{\text{dia}} \rangle$  up to 1.8% at  $B_t \leq 1\text{T}$ . An example of this type of ETB plasma is shown in Fig.3, where the saturation time  $\tau_{\text{sat}}$  of  $\langle \beta_{\text{dia}} \rangle$  (or the stored energy) is  $\sim 350\text{ms}$  and the values of  $\langle \beta_{\text{dia}} \rangle$  and  $\langle n_e \rangle$  at the transition are  $\sim 1.5\%$  and  $1.2 \times 10^{19} \text{ m}^{-3}$ , respectively. In this shot, edge MHD modes with  $m/n=1/2, 2/3, 2/4$  and  $2/5$  slowly grow. This type of an ETB plasma provides an opportunity to study characteristics of ETB plasma in LHD, minimizing impacts of edge MHD instabilities. We have summarized the data of  $\tau_{\text{sat}}$  for various ETB plasmas in LHD. Dependences of  $\tau_{\text{sat}}$  on line averaged electron density  $\langle n_e \rangle$  and  $\langle \beta_{\text{dia}} \rangle$  at the transition are respectively shown in Figs. 4(a) and 4(b). When  $\langle n_e \rangle$  at the L-H transition is less than  $\sim 1.5 \times 10^{19} \text{ m}^{-3}$ , the time of the saturation  $\tau_{\text{sat}}$  is extended more

than 100 ms which is longer than the global energy confinement time. Figure 4(b) clearly indicates that the transition at  $\langle \beta_{\text{dia}} \rangle$  larger than 2% leads to a quick saturation of  $\langle \beta_{\text{dia}} \rangle$ , of which time scale is less than the global energy confinement time.

The changes of electron temperature and

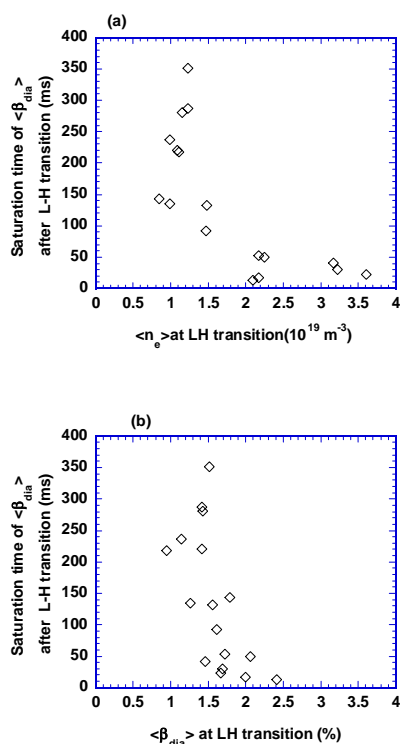


Fig.4 (a) Dependence of the saturation time on  $\langle n_e \rangle$  at the transition, where  $R_{\text{ax}}=3.55\text{m}$  and  $3.6\text{m}$ ,  $|B_t|=0.5\text{-}1.5\text{T}$  and  $P_{\text{abs}}=2\text{-}10 \text{ MW}$ . The saturation time is enhanced significantly in the low density regime of  $\langle n_e \rangle \leq 1.5 \times 10^{19} \text{ m}^{-3}$ . (b) Dependence of the saturation time on  $\langle \beta_{\text{dia}} \rangle$  at the transition. When  $\langle \beta_{\text{dia}} \rangle$  at the transition exceeds  $\sim 2\%$ , the saturation time becomes less than the energy confinement time.

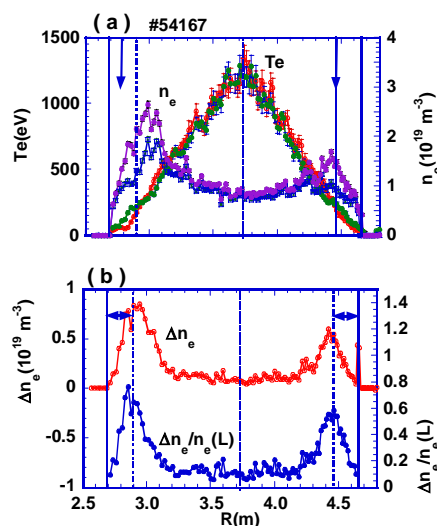


Fig.5 (a) Radial profiles of electron temperature and density just before and after the L-H transition in the configuration of  $R_{\text{ax}}=3.6\text{m}$  and  $\gamma=1.22$  at  $B_t=-0.75\text{T}$ . (b) Radial profile of the increment of electron density across the transition.

density profiles across the transition in relatively low beta H-mode plasma are shown in Fig.5 (a), where R stands for the major radius in the horizontally elongated section of LHD. Electron density and its gradient in the edge region increase noticeably across the transition, while electron temperature profile remains unchanged. Two solid vertical arrows in this figure indicate the position of the last closed flux surface (LCFS) defined in the vacuum field. Two horizontal arrows in Fig.5(b) indicate the width of ETB  $\Delta_{\text{ETB}}$ . In this paper, we call the ‘‘ETB width’’ instead of the ‘‘pedestal width’’, because the electron density profile after the transition does not have a shape of the pedestal observed in tokamak H-modes. The width is defined from the position where the maximum rise in edge electron density is achieved. The formed ETB obviously extends into the ergodic field layer outside the LCFS. Formation of ETB in ergodic field layer suggests considerable radial diffusion in collisional plasma rather than that parallel to the magnetic field line. The width of ETB  $\Delta_{\text{ETB}}$  is in the range of 8 cm to 16 cm for the averaged minor plasma radius  $\langle a \rangle \sim 60$  cm, and has no clear dependence on the toroidal field strength  $B_t$  over 0.5T to 1.5 T, where the rotational transform at ETB is fixed and the poloidal field strength is proportional to  $B_t$  (Fig.6). It should be noted that the ETB width is evaluated as a value averaged over the magnetic surface. The width is often compared with poloidal ion gyro-radius through the scan of the toroidal field strength and/or plasma current in tokamak H-modes [17]. In ETB plasma of LHD, the ETB width is much larger than the poloidal ion gyro-radius  $\rho_{0i}$  where  $\rho_{0i}$  is estimated to be  $\sim 1.2$  cm on the assumption of  $T_e \sim T_i = 0.2$  keV in the H-mode plasmas at  $B_t = 1$ T.

Above-mentioned fairly large width of ETB may be responsible for neutral penetration from the divertor target plates. Calculated neutral penetration for an LHD plasma using a Monte Carlo code having edge plasma parameters of  $5 \times 10^{18} \text{ m}^{-3}$  and  $T_e = 10 \text{ eV}$  is less than 10cm from the outermost layer of ergodic field layer [18, 19]. This suggests neutrals cannot penetrate deeply inside the formed ETB and would not play an essential role in determining the ETB width on LHD, although the detailed calculation of neutral transport in a more realistic magnetic configuration is needed. A thick ergodic field layer is expected to have an effective screening effect for neutral penetration. The other plausible candidate factor for an expanded width of ETB may be ELM activities and/or edge MHD modes [20]. In LHD, ETB width may be affected by destabilization of resistive interchange modes in ETB region, but clear evidence has not been recognized so far. Nevertheless, these data of ETB width would contribute to the database of the pedestal width in tokamak H-mode plasmas.

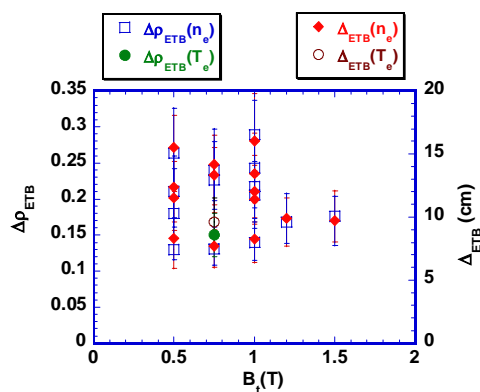


Fig.6 Dependence of the width of ETB ( $\Delta_{\text{ETB}}$ ) derived from electron temperature and density profiles and the width normalized by the averaged minor plasma radius ( $\Delta\rho_{\text{ETB}}$ ) on the toroidal field strength  $B_t$ .

Independently of the ETB plasmas with quick and slow saturation of  $\langle\beta_{\text{dia}}\rangle$  after the transition, the improvement of energy confinement time is modest ( $< 15\%$ ), compared to the ISS95 international stellarator scaling [21], because appreciable density rise takes place by the transition instead of temperature rise in plasma edge. An ETB plasma under the condition of suppressed particle fueling is strongly required to raise the confinement improvement further. The threshold power for the L-H transition is almost the same as the ITER power threshold scaling [22].

### 3. Effects of applied resonant helical field perturbations on ETB formation

The LID coils can generate helical field perturbations resonate with the rational surface of  $1/2\pi=1$  near the edge. The Poincaré plot of field structure is shown in Fig.1(b) for the case that the LID field is applied to expand the  $m/n=1/1$  magnetic island. In this case, ergodic field layer exists outside the sizable  $m/n=1/1$  magnetic island and appreciably expands toward the island separatrix, compared to the case without the island (Fig.1(a)).

In the shot A shown in Fig.7 where the line averaged electron density was ramped up by gas puffing, the L-H transition occurred at  $\langle n_e \rangle \sim 2 \times 10^{19} \text{ m}^{-3}$  and  $\langle\beta_{\text{dia}}\rangle \sim 1.8\%$ . In this shot small LID field was applied to diminish  $m/n=1/1$  magnetic island and the electron

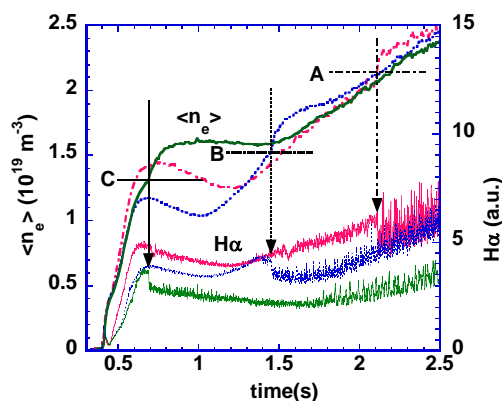


Fig.7 Time evolutions of line averaged electron density and  $H\alpha$ -emission in ETB plasmas with different LID coil current  $I_{\text{LID}}$  at  $B_t=0.75\text{T}$ , where  $I_{\text{LID}}$  are  $-211\text{A}$ ,  $-714\text{A}$  and  $-813\text{A}$  for three shots A, B and C, respectively. Vertical arrows indicate the transition for each shot, and horizontal bars indicate the electron density at the transition. In the shot C, sizable magnetic island is clearly generated on electron temperature profile.

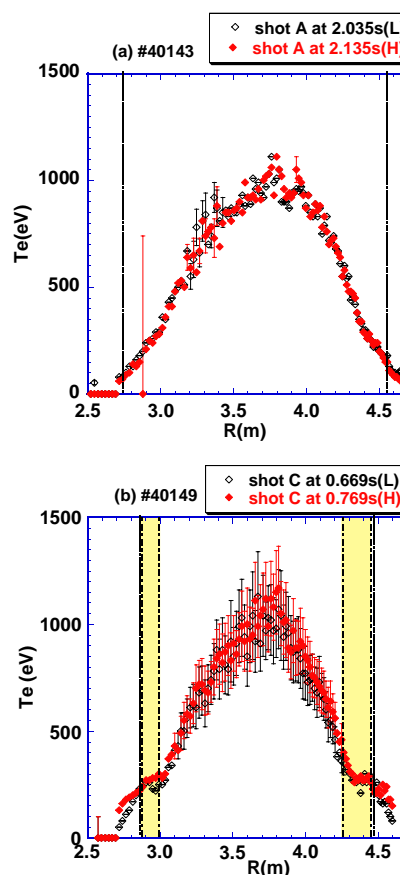


Fig.8 Electron temperature profiles just before and after the L-H transition in the shot A without expanded  $m/n=1/1$  island (LID current  $I_{\text{LID}}=-211\text{A}$ ) (a) and the shot C with expanded island by the LID field ( $I_{\text{LID}}=-813\text{A}$ ) (b). Dotted vertical lines indicate the last closed flux surface in the vacuum field. In Fig.8(b), two dash-and-dot lines indicate the separatrix of the expanded  $m/n=1/1$  island in the vacuum field.

temperature profile did not have any obvious island structures near the edge (Fig.8(a)). When the LID field was increased to expand the size of  $m/n=1/1$  magnetic island near the edge with the same gas puffing (from the shot B to shot C in Fig.7), the transition occurred at lower electron density (for instance,  $\sim 1.3 \times 10^{19} \text{ m}^{-3}$  in the shot C). The ETB was formed outside the expanded island separatrix which slightly moves outward from the location calculated in the vacuum field due to finite beta effect, and considerably extends into the ergodic field layer (Fig.8(b)). Formation of modest electron temperature pedestal in this case may be caused by the transition at lower electron density. However, the sizable  $m/n=1/1$  island degrades core plasma confinement and leads to the decline of  $\langle \beta_{\text{dia}} \rangle$ . If the  $\langle n_e \rangle$  dependence in the ITER power threshold scaling is taken into account [22], the absorbed NBI power at the transition normalized by  $\langle n_e \rangle^{0.64}$  is almost same for three cases with the LID coil current -211A, -714A and -813A. A reason why the transition is triggered at lower  $\langle n_e \rangle$  in the case with a sizable island is not clarified yet.

As seen from Fig.7, ELM like activities in  $\text{H}\alpha$  emission were suppressed by application of large LID field. Moreover, amplitude of coherent  $m/n=2/3$  edge MHD mode was also reduced noticeably. A possible cause of suppression of ELM like  $\text{H}\alpha$  fluctuations and  $m/n=2/3$  edge MHD mode may be the reduction of the pressure gradient at the rational surface  $\iota/2\pi=3/2$  due to expansion of sizable magnetic island. In this experimental campaign, steep pressure gradient region moves outward, but it does not excite other edge MHD modes such as  $m/n=1/2$  of which rational surface resides further outside the  $\iota/2\pi=3/2$  surface.

#### 4. Summary

In helical divertor configuration of LHD, ETB was formed through L-H transition in relatively high beta plasma at  $B_t=0.5\text{T}$  to  $1.5\text{T}$ , where  $R_{\text{ax}}=3.55\text{m}$  and  $3.6\text{m}$ . ETB region extends into ergodic field layer. This fact is interpreted that edge plasma diffuses radially into ergodic field layer, because ETB region is collisional and the mean free path is much shorter than the connection length of magnetic field lines there. An important point is that steep pressure gradient can be realized even in ergodic field layer of thus collisional plasma. We need further study interplay between ETB formation and ergodic field layer. Generation of sizable magnetic island near the edge by application of resonant helical field perturbations leads to the transition at lower electron density and suppression of edge MHD modes and ELM like activities. The width of ETB has no obvious dependence on the toroidal field strength over  $0.5\text{T}$  to  $1.5\text{T}$  and much larger than poloidal ion gyro-radius. Effects of ELM like activities and edge MHD modes on broadening the ETB width should be studied, in addition to detailed evaluation of neutral penetration. Effect of ergodic field layer on ELM activities is also not clarified yet. Actually, ETB plasmas of LHD discussed in this paper have ELM like activities with small amplitude and relatively high frequency. These characters of ELM like activities would not be straightforwardly explained by the formation of ETB in ergodic field layer. A character of ETB that is in the magnetic hill and susceptible of resistive interchange instabilities may control ELM like activities.



Future important issues on ETB formation and control of edge MHD modes/ELM like activities in LHD are following:

- (1) Realization of L-H transition and ETB formation in low collisionality plasmas where ergodic field layer may play a crucial role: application of LID field may be helpful.
- (2) Measurements of plasma parameters and their fluctuations in edge region, having high spatial and time resolutions: they are indispensable to clarify the role of ergodic field layer in ETB plasmas.
- (3) Improved stability of ETB region by plasma effects such as ion diamagnetic and ExB shear flows.

### Acknowledgements

This work is supported in part by the LHD project budget (NIFS05ULHH508) and the Grant-in-Aid for Scientific Research (A) from JSPS, No. 15206107.

### References

- [1] ITER Physics Expert Groups on Conf. and Transport, and Conf. Modeling and Database, Chap.2 of ITER Physics Basis, Nucl. Fusion **39**(1999) 2175, and references therein.
- [2] TOI, K., et al., 14<sup>th</sup> IAEA Conf. On Plasma Phys. Control. Fusion Res. 1992 (Würzburg, 1992), Vol.2(Vienna, IAEA) p461.
- [3] TOI, K., et al., Plasma Phys. Cont. Fus. **38**(1996) 1289.
- [4] OKAMURA, S., et al., Plasma Phys. Cont. Fus. **46**(2004) A113.
- [5] TAKEUCHI, M., et al., Plasma Phys. Cont. Fus. **48**(2006) A277.
- [6] ERCKMAN, V., et al., Phys. Rev. Lett. **70** (1993)2086.
- [7] WAGNER, F., et al., Plasma Phys. Control. Fusion **36**(1994) A61.
- [8] LOARTE, A., et al., Plasma Phys. Control. Fusion **45**(2003)1549.
- [9] EVANS, T.E., et al., Phys. Rev. Lett. **92**(2004) 235003.
- [10] TOI, K., et al., Nucl. Fusion **44**(2004)217.
- [11] TOI, K., et al., Phys. Plasmas **12**(2005)020701.
- [12] TOI, K., et al., Plasma Phys. Control. Fusion **48**(2006)A295.
- [13] MORITA, S., et al., Plasma Phys. Control. Fusion **48**(2006)A269.
- [14] KOMORI, A., et al., Proc. 15th IAEA Conf. Plasma Phys. Control. Fusion Res. (seville, 1994) Vol.2 (Vienna, IAEA)p773.
- [15] ICHIGUCHI, K., et al., Nucl. Fusion **36**(1996)1145.
- [16] GREENFIELD, C.M., et al., Phys. Rev. Lett. **86**(2001) 4544.
- [17] HATAE, T., et al., Plasma Phys. Control. Fusion **40**(1998) 1073.
- [18] SHOJI, M., et al., J. Nucl. Mater. **337-339**(2005) 186.
- [19] TANAKA, K., et al., Nucl. Fusion **46**(2006) 110.
- [20] HATAE, T., et al., Plasma Phys. Control. Fusion **41**(1999) 1371.
- [21] STROTH, U., et al., Nucl. Fusion **36** (1996) 1063.
- [22] ITPA Conf. & H-mode threshold database working group, 19<sup>th</sup> IAEA Fusion Energy Conf. (Lyon, France, 2002) paper No. CT/P-04.